

TITLE: Anthropogenic nitrogen inputs and impacts on oceanic N₂O fluxes in the northern Indian Ocean: the need for an integrated observation and modelling approach

For submission to : DSR II Special Issue on IIOE-2

Revision : Jan. 15th, 2019

AUTHORS : Parvatha Suntharalingam^{1*}, Lauren M. Zamora^{2,3}, Hermann W. Bange⁴, Srinivas Bikkina⁵, Erik Buitenhuis¹, Maria Kanakidou⁶, Jean-Francois Lamarque⁷, Angela Landolfi⁴, Laure Resplandy⁸, Manmohan M. Sarin⁵, Sybil Seitzinger⁹ and Arvind Singh⁵

AFFILIATIONS :

1: School of Environmental Sciences, University of East Anglia, UK.

2 : Earth System Science Interdisciplinary Center (ESSIC), University of Maryland, College Park, MD, USA

3 : NASA Goddard Space Flight Center, Greenbelt, MD, USA

4: GEOMAR Helmholtz Centre for Ocean Research, Kiel, Germany

5: Geosciences Division, Physical Research Laboratory, Ahmedabad, India

6: Environmental Chemical Processes Laboratory, Department of Chemistry, University of Crete, Greece.

7 : National Center for Atmospheric Research, Boulder, CO, USA.

8 : Princeton University, Department of Geosciences and Princeton Environmental Institute, Princeton, USA.

9 : Pacific Institute for Climate Solutions, University of Victoria, Victoria, Canada.

*Corresponding author: P.Suntharalingam@uea.ac.uk

Keywords : nitrous-oxide; nitrogen cycle; air-sea interaction; atmospheric chemistry

Declarations of interest: none

1 ABSTRACT

2 Anthropogenically-derived nitrogen input to the northern Indian Ocean has
3 increased significantly in recent decades, based on both observational and model-
4 derived estimates This external nutrient source is supplied by atmospheric
5 deposition and riverine fluxes, and has the potential to affect the vulnerable
6 biogeochemical systems of the Arabian Sea and Bay of Bengal, influencing
7 productivity and oceanic production of the greenhouse-gas nitrous-oxide (N₂O). We
8 summarize current estimates of this external nitrogen source to the northern Indian
9 Ocean from observations and models, highlight implications for regional marine N₂O
10 emissions using model-based analyses, and make recommendations for
11 measurement and model needs to improve current estimates and future predictions
12 of this impact. Current observationally-derived estimates of deposition and riverine
13 nitrogen inputs are limited by sparse measurements and uncertainties on accurate
14 characterization of nitrogen species composition. Ocean model assessments of the
15 impact of external nitrogen sources on regional marine N₂O production in the
16 northern Indian Ocean estimate potentially significant changes but also have large
17 associated uncertainties. We recommend an integrated program of basin-wide
18 measurements combined with high-resolution modeling and more detailed
19 characterization of nitrogen-cycle process to address these uncertainties and
20 improve current estimates and predictions.

21
22
23 1. INTRODUCTION

24 The 2nd International Indian Ocean Expedition program [Hood et al. 2016] was
25 launched in December 2015 on the occasion of the 50th anniversary of the first
26 International Indian Ocean Expedition program (1959-1965) as a joint effort of the
27 Scientific Committee on Oceanic Research (SCOR), the Intergovernmental
28 Oceanographic Commission (IOC) and the Indian Ocean Global Observing System
29 (IOGOOS). IIOE-2 was set up to advance Indian Ocean initiatives and projects
30 addressing emerging scientific issues of the Indian Ocean in the 21st century. To this
31 end, a deeper understanding of the biogeochemical and socio-economic feedbacks
32 associated with ongoing changes in the Indian Ocean is critical to better project and
33 mitigate the consequences of the anthropogenic activities for the Indian Ocean
34 region and beyond.

35 The biogeochemical systems of the northern Indian Ocean are vulnerable to
36 the increasing levels of bioavailable reactive nitrogen derived from human activities
37 (e.g., fossil-fuel combustion, agriculture) and supplied to the coastal and open ocean
38 through atmospheric pollution outflow and riverine inputs [von Glasow et al. 2013;
39 Ramanathan et al. 2005; Duce et al. 2008; Seitzinger et al. 2010]. These external
40 inputs of reactive nitrogen provide an additional nutrient source to marine
41 ecosystems and can have significant impacts on regional biological productivity and
42 the associated generation of greenhouse gases such as nitrous oxide (N₂O). The
43 activities of the Joint Group of Experts on the Scientific Aspects of Marine
44 Environmental Protection (GESAMP) Working Group 38 on the Atmospheric Input of
45 Chemicals to the Ocean (<http://www.gesamp.org/work/groups/38>) have previously
46 highlighted the increasing levels of anthropogenically derived nitrogen provided to
47 global ocean ecosystems via atmospheric deposition and riverine fluxes, and their

48 the potentially complex impacts on these ecosystems (e.g., Duce et al. 2008;
49 Dentener et al. 2006; Suntharalingam et al. 2012; Jickells et al. 2017). The northern
50 Indian Ocean, in particular, was noted to be a region subject to high and rapidly
51 increasing anthropogenic nitrogen deposition [Dentener et al. 2006; Baker et al.
52 2017], and the resulting impacts on local ocean biogeochemistry are poorly
53 characterized. This commentary results from GESAMP Working Group 38 activities to
54 examine these regional impacts in the northern Indian Ocean, and in particular, to
55 assess implications for oceanic emissions of the greenhouse gas nitrous-oxide (N_2O);
56 the Arabian Sea region is a known site of dynamic N_2O cycling [Bange et al. 2001;
57 Naqvi et al. 2006, 2010a]. In this study we provide a synthesis of current estimates
58 of sources of external nitrogen inputs to the northern Indian Ocean, and discuss the
59 implications for regional oceanic emissions of N_2O using existing estimates from
60 global model analyses and a new estimate based on a high-resolution model of the
61 Indian Ocean. An important aim of this commentary is to highlight much needed
62 advances in regional observations and model analyses to achieve more reliable
63 estimates of current and future N_2O emissions in this region.

64

65 **Nitrous oxide in the northern Indian Ocean**

66 Oceanic N_2O production and consumption pathways display significant sensitivity to
67 the ambient dissolved oxygen level [Codispoti et al. 2001; Bange et al. 2010]. In well-
68 oxygenated waters, N_2O is produced during nitrification processes involving the
69 microbial oxidation of ammonia to nitrate [Cohen and Gordon, 1979]. Culture
70 studies indicate enhanced yields associated with decreasing ambient oxygen levels
71 [Goreau et al. 1980; Frame and Casciotti, 2010; Löscher et al., 2012]. In suboxic and
72 anoxic waters, denitrification processes dominate, and N_2O is formed as an
73 intermediate product of the microbial reduction of nitrate to nitrogen gas during
74 organic matter remineralization (i.e., incomplete denitrification) [Naqvi et al. 2000].
75 As ambient oxygen levels approach anoxia, N_2O can be further reduced to N_2 , thus
76 denitrification processes also provides a sink of N_2O at very low oxygen levels. The
77 turnover of N_2O at the sub-oxic to oxic interface of low oxygen waters is observed to
78 be highly dynamic, with gross production and consumption fluxes significantly larger
79 (~20 times) than the residual net N_2O yield from incomplete denitrification [Babbin
80 et al. 2015].

81 N_2O production and the underlying nitrogen cycling mechanisms in the
82 northern Indian Ocean (defined here as the Indian Ocean region located north of the
83 Equator) are fundamentally influenced by the unique characteristics of the region's
84 oceanic circulation and associated biogeochemistry. This region encompasses the
85 Arabian Sea and the Bay of Bengal and hosts two of the most intense oxygen
86 minimum zones (OMZs) worldwide [Paulmier and Ruiz-Pino, 2006; Morrison et al.
87 1999; Bristow et al. 2017]. The extensive Arabian Sea OMZ is a region noted for
88 intense denitrification [Naqvi et al. 2006; Ward et al. 2009], and a 'hotspot' for
89 generation of marine N_2O [Naqvi et al. 2010a]. Production rates of N_2O here are
90 hypothesized to reach 10,000 times the ocean average [Codispoti, 2010]. In
91 contrast, although widespread low oxygen levels have been reported in the Bay of
92 Bengal [e.g., submicromolar O_2 , Bristow et al. 2017], extensive anoxia and
93 denitrification have not been detected here, possibly due to the persistence of trace
94 levels of oxygen that inhibit this process [Bristow et al. 2017]. The large riverine

95 freshwater discharge in the north of the Bay of Bengal from the Ganges outflow, in
96 conjunction with riverine discharge from the peninsular subcontinent into the south-
97 west of the Bay of Bengal has resulted in a latitudinal gradient in surface N₂O
98 concentrations along the coast of the western Bay of Bengal characterized by
99 equilibrium or under-saturation in the northwest of the basin and small
100 supersaturation and emission in the south-west [Rao et al. 2013]. According to Rao
101 et al. [2013] this complex behavior results from a combination of factors, including
102 seasonal undersaturation in N₂O associated with monsoonally-governed variations in
103 Ganges freshwater outflow, and higher nitrification rates and associated N₂O
104 supersaturation in the coastal upwelling regions in the south-west of the Bay of
105 Bengal.

106 The Asian monsoon system plays an important role in regulating the
107 temporal variation of the region's N₂O production and emission to the atmosphere.
108 Monsoonal winds drive a seasonally reversing upper ocean circulation with
109 associated changes in seasonal upwelling and regional biological productivity in both
110 the Arabian Sea and the Bay of Bengal [McCreary et al., 2013; Schott and McCreary,
111 2001; Madhuratap et al. 1996, and references therein]. This upwelling is most
112 intense in the NW Arabian Sea and leads to especially high regional N₂O [De Wilde
113 and Helder, 1996; Bange et al. 2001]. The Asian monsoon system also accounts for
114 pronounced rainfall and river discharge in the northern Bay of Bengal, playing an
115 important role in the hydrography and associated biogeochemistry of the basin.
116 These freshwater fluxes reduce surface salinity and enhance water column
117 stratification, yielding lower productivity levels in the Bay of Bengal than in the
118 neighbouring Arabian Sea [Rao et al. 2013; Singh and Ramesh, 2015 and references
119 therein].

120 Previous estimates of oceanic N₂O emission from the northern Indian Ocean
121 highlight its significant contribution to global fluxes [Law and Owens 1990; Naqvi and
122 Noronha 1991; Lal and Patra 1998; Bange et al. 2001]. The Arabian Sea, in particular,
123 is a region of intense oceanic N₂O production, and is estimated to provide a flux to
124 the atmosphere of 0.2 – 0.6 Tg N yr⁻¹ [Naqvi et al., 2010b]. This flux represents 2 – 31
125 % of global total oceanic N₂O emissions (N₂O emissions (1.9 – 12.3 Tg N yr⁻¹) from
126 the open ocean, coastal and estuarine sources [Ciais et al. 2013]. In contrast N₂O
127 fluxes to the atmosphere from the Bay of Bengal are considerably lower (0.027 -
128 0.077 Tg N yr⁻¹) [Naqvi et al. 1994; Naqvi et al. 2010a], a result of less pronounced
129 upwelling and lower productivity levels.

130

131 **Vulnerability to climate change and anthropogenic nutrient input**

132 The circulation and biogeochemistry of the northern Indian Ocean basins are
133 vulnerable to the impacts of climate warming and associated changes; for example,
134 to (a) ocean deoxygenation and the predicted expansion of ocean OMZs [Stramma et
135 al. 2010; Naqvi et al. 2010b; Banse et al 2014], and (b) potential increases in the
136 intensity of the monsoonal circulation and associated upwelling and productivity in
137 the Arabian Sea [De Castro et al. 2016; Goes et al. 2005]. Such changes could result
138 in significant increases in oceanic N₂O emissions from the region [Codispoti, 2010].
139 These hypotheses are supported by recent model analyses that predict the
140 deepening and intensification of the Arabian Sea OMZ due to strengthening of the
141 region's monsoonal winds [Lachkar et al. 2018], and increases in northern Indian

142 Ocean N₂O production associated with expansion of oceanic low-oxygen regions
143 under scenarios of 21st century warming [Martinez-Rey et al. 2015]. A key
144 vulnerability of the Bay of Bengal results from the observed widespread low oxygen
145 levels. The regional biogeochemical system is on the brink of hypoxia, and further
146 oxygen depletion (via physical or biological forcing) could tip this ocean region into a
147 regime of denitrification with significant increases in N₂O and N₂ emission to the
148 atmosphere [Naqvi et al. 2008; Bristow et al. 2017].

149 N₂O emissions from the Arabian Sea and the Bay of Bengal could also
150 respond to the rapidly rising supply of anthropogenically-derived nutrient inputs to
151 these basins [Naqvi et al. 2010a]. Nutrient supply (of N, P, Si, Fe) to marine
152 ecosystems has increased significantly over the past century; this increase is
153 projected to continue in the future due to higher levels of fossil fuel combustion,
154 agricultural fertilizer application, and dust mobilization through land-use change
155 [Duce et al., 2008; Seitzinger et al. 2010; Fowler et al. 2013; Sattar et al., 2014].
156 Previous global-scale analyses of the impact of increasing anthropogenic nitrogen
157 inputs estimate that highest impacts will occur on ocean ecosystems in coastal
158 regions downwind of atmospheric pollution outflow and influenced by riverine
159 discharge [Doney et al. 2007; Krishnamurthy et al. 2007; Seitzinger et al. 2010]. Such
160 increases in nitrogen inputs are predicted to influence marine productivity, organic
161 matter export and remineralization, and cause coastal eutrophication [Galloway et
162 al. 2003; Gruber and Galloway, 2008]. These changes will also have an impact on the
163 oceanic N₂O source by influencing the magnitude of regional nitrification and
164 denitrification fluxes, and by altering the extent of hypoxic and sub-oxic regions
165 where N₂O production yields are higher than in the oxic ocean [Duce et al. 2008].
166 Analyses of the impacts of increases in nutrient deposition on productivity have
167 highlighted the potential for especially high impacts in the northern Indian Ocean
168 [Naqvi et al., 2000; 2009; Capone and Hutchins, 2013; Suntharalingam et al. 2012].
169 This region is also noted to be vulnerable to marine nitrogen cycle feedbacks,
170 whereby relatively small nitrogen inputs from atmospheric nitrogen deposition could
171 increase local rates of denitrification and cause large net nitrogen losses [Somes et
172 al. 2016; Yang and Gruber 2016; Landolfi et al. 2017].

173 Current estimates of the anthropogenic nitrogen supply to the northern
174 Indian Ocean and its impact on the region's ecosystems and biogeochemistry are
175 derived from sparse measurements and a limited set of model analyses. In this
176 commentary, we bring together recent estimates of external nitrogen inputs to the
177 Arabian Sea and Bay of Bengal from atmospheric deposition and riverine sources
178 (section 2). We also discuss the implications of this additional nutrient source for
179 oceanic N₂O production in the northern Indian Ocean based on (i) a synthesis of
180 previous global ocean biogeochemistry model studies (section 3.1), and (ii) a newly-
181 derived estimate of Arabian Sea N₂O production using a regional high-resolution
182 model (section 3.2). We discuss key uncertainties in these model estimates (sections
183 3.3 and 3.4), and highlight the need for a comprehensive and integrated
184 measurement and modeling effort towards more reliable prediction of future
185 changes in N₂O emissions from the northern Indian Ocean (section 4).

186

187

188

189 2. Inputs of externally derived nitrogen to the northern Indian Ocean

190 There has been an approximately 12-fold increase in the rates of Indian agricultural
191 nitrogen fertilizer consumption since the 1970s associated with rapid economic
192 development [Ramesh et al. 2007]. Some part of this increased nitrogen load on
193 land is transported into the northern Indian Ocean's estuaries and coastal waters
194 (e.g., Martin et al. [2011]; Singh and Ramesh [2011]; Krishna et al. [2016]) likely
195 resulting in rapid increases in aquatic organic and inorganic nitrogen levels [Liu et al.
196 2008]. Based on results from the Global Nutrient Export from WaterSheds (NEWS)
197 model [Pedde et al. 2017; Seitzinger et al. 2010], we estimate that there was an
198 ~50% ($1.22 \text{ Tg N yr}^{-1}$) increase in riverine dissolved nitrogen input into the northern
199 Indian Ocean between 1970-2000, 87% of which was directed into the Bay of Bengal.

200 Atmospheric chemistry models also estimate substantial increases in
201 atmospheric nitrogen deposition to the northern Indian Ocean over recent decades
202 [Dentener et al. 2006; Kanakidou et al. 2012, 2016; Lamarque et al. 2013]. This trend
203 is supported by observations; e.g., since the 1980s, NO_x emissions over India have
204 more than doubled [Garg et al. 2006], and there have been significant increases in
205 observed wet nitrate deposition at different coastal and open ocean sites [Attri and
206 Tyagi, 2010; Safai et al., 2004]. Cruise measurements made between 2001-2009 in
207 the Bay of Bengal show similar trends for aerosol NH_4^+ concentrations [Srinivas et al.,
208 2011]. Based on a combination of output from the NCAR-CAM (version 3.5) model
209 [Lamarque et al., 2011] and the TM4-ECPL model [Kanakidou et al., 2012] models
210 (see Appendix A for details), we estimate an ~226% (1.42 Tg N m^{-2}) increase in the
211 amount of soluble nitrogen being deposited to the northern Indian Ocean between
212 1850 and 2005, 59% of which went into the Arabian Sea.

213 Table 1 presents estimates of the relative contribution of external (i.e., non-
214 recycled) soluble nitrogen sources to the present-day northern Indian Ocean. The
215 sources and calculation methods for these estimates are described in Appendix A.
216 The inorganic nitrogen inputs are in line with previous estimates derived from
217 models, including those here used [Dentener et al., 2006; Kanakidou et al., 2012,
218 2016; Lamarque et al., 2013; Vet et al., 2014] and ground-based observations [Baker
219 et al., 2017; Singh et al., 2012; Srinivas et al., 2011; Srinivas and Sarin, 2013]. Note
220 that models and observations are not always directly comparable, as the models do
221 not represent all processes with sufficient accuracy, and the observations do not
222 provide comprehensive spatial and temporal coverage. The estimates of Table 1
223 suggest that recent rapid increases in riverine and atmospheric nitrogen are non-
224 negligible influences on the external nitrogen fluxes to these ocean basins.

225 For biologically-mediated nitrogen sources, there are very few estimates of
226 nitrogen (N_2) fixation in the northern Indian Ocean. Direct estimates, made using
227 isotopically enriched ($^{15}\text{N}_2$) tracers, suggest extremely high rates of N_2 fixation in the
228 Arabian Sea during springtime (Table 1, Gandhi et al., 2011). Srinivas and Sarin
229 [2013] provide indirect estimates of N_2 fixation rates, derived with respect to
230 atmospheric deposition inputs and assuming Fe and P limitation in the ocean; these
231 estimates suggest a large variability in regional N_2 fixation rates, linked to the
232 uncertainty in atmospheric deposition fluxes. The role of N_2 fixation must also,
233 therefore, be better constrained for a more accurate assessment of anthropogenic
234 nutrient impacts on the biogeochemistry of the northern Indian Ocean.

235

236

237 Uncertainties in nitrogen inputs

238 Data available to validate model estimates for the region are still sparse, particularly
239 for the Bay of Bengal. For example, we found references to only three cruises that
240 sampled aerosol water soluble organic nitrogen (WSON) (compiled in Srinivas et al.,
241 [2011] and Srinivas and Sarin [2013]). Inorganic dry nitrogen deposition is better
242 constrained, with over 400 individual ship-based observations, but sample sizes are
243 still insufficient to adequately characterize the north Indian Ocean's high inter-
244 annual and seasonal variability, and the expected increases in deposition with time
245 (e.g., more than half of the observations were collected prior to the year 2000).
246 There are particularly high uncertainties in wet deposition estimates due to small
247 numbers of observations over the open ocean.

248 As with atmospheric and riverine inputs, observations of N_2 fixation to the
249 Arabian Sea are also sparse, particularly over the Bay of Bengal, where there have
250 only been a few reports of rates from *Trichodesmium* [Jyothibabu et al., 2017]. The
251 relatively low number of observations for the different external nitrogen sources
252 makes it challenging to validate regional models, resulting in high uncertainties in
253 descriptions of the mean system state. The paucity of the data, along with rapid and
254 large-scale increases in anthropogenic nutrient inputs, highlight the need for a more
255 detailed evaluation of external nutrient inputs to the region.

256

257 3. Implications for oceanic N_2O production in the northern Indian Ocean

258 **3.1 Estimates from global models:** The impacts of increasing levels of
259 anthropogenically derived atmospheric nitrogen deposition on marine
260 biogeochemistry and N_2O production have been investigated by recent ocean
261 biogeochemistry model analyses (e.g., Suntharalingam et al. [2012], Jickells et al.
262 [2017], Landolfi et al. [2017]). While these studies estimate relatively modest
263 increases in oceanic N_2O production at the global scale (1-3%), they all suggest more
264 significant regional impacts in regions of high nutrient deposition downwind of
265 continental outflow in the vicinity of oceanic OMZs. In particular, the northern
266 Indian Ocean, and specifically the Arabian Sea, is noted as one of the most sensitive
267 regions to changes in this anthropogenic nutrient input. Table 2 summarizes
268 estimated changes in N_2O production in the northern Indian Ocean from the above
269 three global model analyses. The ocean biogeochemical models include ecosystems
270 of varying complexity, but all represent marine cycles of carbon, nitrogen,
271 phosphorus, oxygen and N_2O . The three model analyses synthesized in Table 2 also
272 employed different model-derived estimates of atmospheric nitrogen deposition to
273 the ocean, which differ in some aspects of flux composition (e.g., organic nitrogen
274 levels, proportion of oxidized and reduced nitrogen species [Jickells et al. 2017]).
275 These details, and the individual ocean model specifications, are given in Appendix B
276 and in the individual publications. Despite differences in their representation of
277 ocean ecosystem processes and nutrient inputs all model analyses estimate
278 increases in surface biological productivity and organic matter export in response to
279 increases in nitrogen deposition from the pre-industrial to the present day. These
280 analyses also estimate proportionately larger changes in N_2O production in the
281 northern Indian Ocean than on the global scale (e.g., increases of 1%-10% for the
282 northern Indian Ocean in comparison to 1%-3% on the global scale). This regional

283 enhancement of N₂O production primarily results from the combination of increased
284 export production resulting from high levels of nitrogen deposition from Indian sub-
285 continental outflow, in conjunction with higher yields of N₂O associated with the
286 Arabian Sea OMZ [Suntharalingam et al. 2012].

287 Limitations of these model-based estimates include potential errors in model
288 circulation arising from the coarse resolution of the global models (i.e., horizontal
289 resolution ranging from 1.5° to 3.7°), and the nitrogen cycle parameterizations
290 employed, which did not always account for more complex interactions and
291 feedbacks. For example, Suntharalingam et al. [2012] report the highest increases in
292 N₂O production (e.g., of over 25% in net N₂O production in the 300-1000 m depth
293 range of the north-eastern Arabian Sea), however, this may be an overestimate, as
294 this model analysis did not account for the potential suppression of N₂ fixation in
295 response to increases in available nitrogen from deposition. The nitrogen cycle
296 dynamics of estuarine and shelf regions (e.g., sedimentary denitrification of riverine
297 nitrogen input) are also not well represented in coarse-resolution models, leading to
298 uncertainties in the impacts of riverine nitrogen on the biogeochemistry of the
299 northern Indian Ocean (see further discussion of nitrogen cycle related uncertainties
300 in section 3.4). Here, we first discuss uncertainties arising from representation of the
301 regional circulation of the northern Indian Ocean in global models.

302 Coarse grid ocean models (e.g., with horizontal resolution > ~1°) are not able
303 to represent the circulation dynamics (i.e., those regulating equatorial currents,
304 lateral mixing and ventilation) that control the extent, intensity and evolution of
305 tropical OMZs [Coco et al. 2013; Bopp et al. 2013; Stramma et al. 2012;
306 Gnanadesikan et al. 2012]. This presents challenges for accurate model simulation of
307 N₂O production and consumption processes in hypoxic, suboxic and anoxic waters,
308 as the nitrification and denitrification processes controlling N₂O production and
309 consumption demonstrate significant sensitivity to even small shifts in local oxygen
310 levels; e.g., shifts of < 5 μmol L⁻¹ in a sub-oxic regime can result in changes from net
311 N₂O production to net consumption via denitrification, thus affecting the region's
312 net N₂O fluxes [Zamora and Oschlies, 2014].

313 Eddy-resolving model analyses (1/12° resolution) of the Arabian Sea [e.g.,
314 Resplandy et al. 2011, 2012; Lachkar et al. 2018] indicate that representation of the
315 mesoscale dynamics at this resolution improves simulation of the region's seasonal
316 biological productivity, associated remineralization, and the position, extent and
317 intensity of the Arabian Sea OMZ. While higher-resolution regional models (< 1°)
318 have previously investigated aspects of the biological productivity and oxygen
319 distribution of the northern Indian Ocean [Wiggert et al. 2000; Resplandy et al. 2011,
320 2012], to our knowledge, the regional nitrogen cycle, and in particular, the impact of
321 nitrogen deposition on oceanic N₂O in the Arabian Sea, has not been investigated at
322 these spatial scales. Below, we use results from a regional high-resolution ocean
323 model to derive a diagnostic estimate of this impact on N₂O; the aim is to highlight
324 the need for more detailed representation of the Arabian Sea's circulation and
325 biogeochemistry when assessing nitrogen cycle changes and predicting the future
326 evolution of N₂O fluxes from this critical region.

327
328

329 **3.2 Estimating Arabian Sea N₂O production with output from a high-resolution** 330 **regional model**

331 We present here a diagnostically derived estimate of oceanic N₂O production in the
332 Arabian Sea, using biogeochemical fluxes and fields from the regional eddy-resolving
333 (1/12° resolution) ocean model of Resplandy et al. [2011, 2012]. In comparison to
334 global coarse resolution models, this high resolution regional model produces an
335 improved representation of the mesoscale variability and circulation of the Arabian
336 Sea (e.g., monsoonal upwelling), and of the local biological productivity. Particularly
337 relevant to N₂O are the good simulation of the regional oxygen distribution (e.g.,
338 ambient concentrations and oxygen utilization rates), and the improved
339 representation of the Arabian Sea OMZ [Resplandy et al. 2011, 2012].

340 Our diagnostic estimate of N₂O production in the Arabian Sea (Figure 1) is
341 derived from the N₂O cycle parameterizations of Suntharalingam et al. [2012]
342 applied to the gridded biogeochemical and flux distributions (specifically oxygen and
343 oxygen utilization rates) of the high-resolution simulations of Resplandy et al. [2012].
344 We estimate gridded fields of N₂O production as the sum of (i) N₂O from nitrification
345 in oxygenated waters, (ii) enhanced N₂O production in low oxygen conditions (via
346 denitrification and enhanced nitrification), and (iii) N₂O consumption in
347 conditions close to anoxia (see Appendix C for calculation details). The model
348 estimate of net N₂O production in the Arabian Sea region is 0.23 Tg N yr⁻¹, with a
349 range of 0.1 - 0.56 Tg N yr⁻¹ when accounting for sensitivity analyses conducted on
350 variations in N₂O yield rates (yields taken from Law and Owens [1990], Naqvi and
351 Noronha [1991], and Patra et al. [1999], see Table C1 in Appendix C). This is
352 consistent with previous observationally-derived estimates of N₂O flux for the
353 Arabian Sea (e.g., 0.2-0.6 Tg N yr⁻¹ [Naqvi et al., 2010a]). We calculate empirically-
354 based estimate of the impact of changes in nitrogen deposition in this region by
355 combining N₂O production estimates from the regional model together with the
356 deposition-induced changes in N₂O yield in the Arabian Sea from the model results
357 of Suntharalingam et al. [2012] (see Appendix C for details of the estimation). We
358 estimate a resulting change in Arabian Sea N₂O production from the pre-industrial to
359 the present of 0.01-0.07 Tg N (the range reflects sensitivity analyses on N₂O yield
360 rates). This corresponds to an estimated increase of 5% - 30% of the Arabian Sea N₂O
361 source. This estimate is derived diagnostically, thus has limited applicability for
362 predictive purposes. However, the relatively large estimated impact, and the large
363 uncertainty, highlights the need to develop high-resolution regional process models
364 of nitrogen and N₂O cycling, that also account for the specific nitrogen-cycling
365 pathways important in low-oxygen regions, in order to more accurately assess the
366 impacts of anthropogenic and climate induced changes in the northern Indian
367 Ocean.

368 369 **3.3 Uncertainties in model representation of the N₂O and nitrogen cycles**

370 The representation of the N₂O cycle in the current generation of global
371 biogeochemical models relies on parameterized functions derived from a relatively
372 limited set of laboratory process studies, and optimized using in-situ oceanic
373 measurements of N₂O and related biogeochemical quantities [Buitenhuis et al. 2018;
374 Battaglia and Joos, 2017; Zamora and Oschlies, 2014; Martinez-Rey et al. 2015;
375 Suntharalingam et al. 2012]. These parameterizations have some success in

376 representing the N₂O distribution in the well-oxygenated ocean where nitrification
377 processes dominate N₂O production. However, global models do not simulate well
378 the complex interplay of N₂O production and consumption pathways, primarily
379 involving denitrification, that regulate N₂O in low oxygen regions such as the Arabian
380 Sea OMZ [Suntharalingam et al. 2000; Martinez-Rey et al. 2015; Zamora and Oschlies
381 2014]. A key model challenge in these regions is the accurate representation of the
382 net N₂O yields resulting from the competing effects of dynamic production and
383 consumption processes at the sub-oxic to anoxic interface, and in simulating the
384 associated steep gradients in N₂O observed at the oxycline boundaries of OMZs
385 [Babbin et al. 2015, Ji et al. 2015; Kock et al., 2016]. The vertical spatial scale of these
386 gradients in N₂O and oxygen at OMZ boundaries are on the order of ~10s of metres,
387 thus their representation remains challenging in the current generation of global
388 biogeochemical models with relatively low spatial resolution.

389 A further challenge for biogeochemical models is the accurate representation
390 of background nitrogen cycle processes (e.g., N₂ fixation), and potential regulation of
391 these processes by changes in external nitrogen sources to marine ecosystems (e.g.,
392 from atmospheric deposition and riverine sources). Observational evidence suggests
393 that N₂ fixation provides an important 'new nitrogen' source to the northern Indian
394 ocean [Table 1 and references therein]. Regional estimates of this source are based
395 on very sparse measurements and have significant uncertainties (see Table 1).
396 Gandhi et al. [2010ab] additionally note significant temporal and spatial variability of
397 the episodic N₂ fixation blooms in the Arabian Sea, and highlight the need for more
398 comprehensive measurements to improve characterization of this nitrogen source
399 and quantification of its magnitude. Previous model analyses have included
400 interactions between nitrogen cycle processes, for example, by accounting for
401 suppression of N₂ fixation in the presence of bio-available nitrogen from deposition
402 [Krishnamurthy et al. 2009; Yang and Gruber 2016; Jickells et al. 2017, Landolfi et al.
403 2017]. However, challenges remain in accurately simulating such interactions, and in
404 representing the role of micronutrients such as iron [Moore and Doney, 2007'
405 Martino et al., 2014; Weber and Deutsch, 2014] in regulating the supply of fixed
406 nitrogen to surface ocean ecosystems.

407 On longer time-scales of decades to centuries, a potentially important
408 feedback process associated with the oxygen depleted basins of the northern Indian
409 Ocean involves the interaction between nitrogen deposition, denitrification and N₂
410 fixation [Landolfi et al. 2013; Somes et al. 2017]. We discuss this in more detail in
411 section 3.4 below.

412

413 **3.4 Implications of increasing nitrogen deposition for changes in water column** 414 **denitrification**

415 While increased nitrogen loading may initially fertilize biological production, the
416 onset of biogeochemical feedbacks may lead to an overall nitrogen impoverishment
417 of the region [Landolfi et al. 2013] with impacts on biological productivity [Somes et
418 al. 2017]. In oxygen deficient regions, increased organic matter production may
419 exacerbate oxygen consumption and stimulate anaerobic remineralization via
420 denitrification, which consumes fixed nitrogen. A simplified analysis combining
421 modeled nitrogen deposition fields with regional oxygen data [Bianchi et al., 2012]
422 suggests that the nitrogen removed by atmospheric nitrogen-driven denitrification

423 may be larger than the nitrogen gain (Figure 2). This is based on the following
424 simplifying assumptions: 1) atmospheric nitrogen deposited onto surface waters
425 overlying the OMZ produces biomass in Redfield ratios and sinks at those locations,
426 2) export flux within the OMZs can be represented either by the standard Martin
427 curve [Martin et al., 1987] or following the fit computed by Van Mooy et al. [2002]
428 from sub-oxic zone regions, 3) organic matter within the OMZ is remineralized under
429 anoxic conditions by denitrification, following 4) standard denitrification
430 stoichiometry [e.g. Paulmier et al. 2009], such that for every mole of nitrogen from
431 organic matter remineralised in sub-oxic waters, up to 7 additional moles of ambient
432 seawater nitrate may be lost to N_2 due to its role as an electron acceptor in the
433 denitrification process [Codispoti et al., 2001]. These assumptions do not account for
434 such factors as advection-driven redistributions of deposited atmospheric nitrogen,
435 any deposition-driven expansion of OMZs and other nitrogen-inventory stabilizing
436 feedbacks, such as the reduction of fixed nitrogen inputs by marine N_2 fixers. These
437 processes have impacts of differing sign and magnitude and may counteract each
438 other. Using the more comprehensive model of Landolfi et al. [2017] we find that
439 following atmospheric deposition of nitrogen in the light-lit surface waters, N_2 fixers
440 lose their competitive advantage (6% decline). The oxygenic remineralization of
441 organic matter at depth promotes the expansion of low-oxygen waters in the
442 Arabian Sea and Bay of Bengal triggering nitrogen loss via water column and benthic
443 denitrification (12% increase). In this model, the increased atmospheric nitrogen
444 load ($+2.7 \text{ Tg N yr}^{-1}$) leads to an additional loss of $0.53 \text{ Tg N yr}^{-1}$, that is a $\sim 10\%$ larger
445 nitrogen-cycle imbalance relative to preindustrial conditions [Landolfi et al. 2017].
446 This highlights a potential negative feedback that acts to stabilize the oceanic
447 nitrogen inventory when subject to additional anthropogenic nitrogen inputs.

448

449 **4. Summary and Recommendations**

450 Nitrogen cycle processes regulating N_2O emissions from the northern Indian Ocean
451 basins are vulnerable to the ongoing rapid increase in the regional outflow of
452 anthropogenically derived nitrogen to the two ocean basins. The Arabian Sea OMZ is
453 currently a globally significant site for oceanic N_2O production, where N_2O emissions
454 could increase under this increased nitrogen loading, especially in conjunction with
455 other climate-induced stressors such as ocean deoxygenation. Biogeochemical
456 systems in regions of the Bay of Bengal are close to hypoxia, and could shift into a
457 denitrifying regime, with loss of N_2O and N_2 to the atmosphere, if oxygen levels are
458 further depleted by biogeochemical or physical drivers. Many of the biogeochemical
459 processes governing these changes are currently poorly characterized by
460 observations, and their representation in models (ocean and atmospheric) have
461 significant uncertainties.

462

463 To enable more accurate estimation of the impacts of anthropogenic nitrogen inputs
464 on current and future N_2O emissions from this region, we recommend further
465 investigation into the following key issues:

466 (1) Reduction of uncertainties on external nitrogen inputs to the northern Indian
467 ocean by :

468 a) improved characterization of the magnitude, composition (i.e., ammonium,
469 nitrate, organic nitrogen), and variability of the atmospheric nitrogen

470 deposition flux to the Arabian Sea and Bay of Bengal. This requires an
471 observational strategy involving regular monitoring of aerosol composition at
472 representative sites, as well as targeted field campaigns to account for
473 monsoonal influences, and to identify the major pathways of pollution
474 outflow from the sub-continent. These data also require consolidation to
475 derive regional atmospheric deposition nitrogen fluxes using high resolution
476 atmospheric modeling. In turn, this requires well calibrated, up-to-date high-
477 resolution emissions of the precursors to nitrogen deposition (such as NO
478 and NH₃ emissions).

479 b) implementation of a long-term nutrient monitoring network in rivers draining
480 into the Arabian Sea and Bay of Bengal. We recommend regular sampling
481 (e.g., monthly) of the outflow of nutrient fluxes, and process studies in
482 estuarine and shelf systems to characterize local nitrogen cycling dynamics
483 and to assess the proportion of riverine nitrogen reaching open ocean
484 waters.

485 c) accurate quantification of the contribution of N₂ fixation to the regional
486 nitrogen budget through a comprehensive program of direct measurements.
487 In addition, improved understanding is required on the processes regulating
488 activity of nitrogen-fixing organisms (for example, concerning potential
489 suppression of activity under nitrogen input from deposition, and regulation
490 by micro- and macro- nutrients).

491

492 2) Improved assessment of the potential impacts of these anthropogenic nitrogen
493 inputs on the regional oceanic N₂O fluxes. This requires:

494 (a) a comprehensive observational approach providing in-situ measurements and
495 process-knowledge to improve current understanding on the evolution of N₂O in the
496 low-oxygen waters of both basins. Such a strategy will include:

497 i. basin-wide networks of regular measurements of nitrogen cycle process rates
498 (e.g., nitrification, denitrification, N₂ fixation) in the water column at selected
499 sites in the Arabian Sea and Bay of Bengal to decipher the short- and long-
500 term trends of the N₂O and background nitrogen cycle.

501 ii. regular time-series measurements of N₂O, oxygen and nutrient depth profiles
502 at representative sites in the coastal and open ocean of the Arabian Sea and
503 the Bay of Bengal.

504 iii. high-resolution measurements of N₂O in the surface ocean and the
505 atmospheric boundary layer on voluntary observing ship (VOS) lines crossing
506 the Arabian Sea and Bay of Bengal.

507 iv. further development of high-spatial-resolution satellite and aircraft
508 observations of near-surface atmospheric nitrogen species (e.g., NO_x and
509 N₂O) and surface-ocean phytoplankton composition, which can be used to
510 evaluate atmospheric deposition and its impacts on marine ecosystems.

511

512

513 (b) A targeted modeling strategy involving :

514 i. development of customized regional biogeochemical process models that
515 build on recent advances in eddy resolving models of the Arabian Sea and
516 Bay of Bengal, and also incorporate the key nitrogen and N₂O cycling

517 processes specific to the region's low-oxygen waters. Specific improvements
518 required to current model parameterizations include accurate
519 characterization of the oxygen thresholds and denitrification processes
520 regulating N₂O production, consumption, and the net yield in the region's
521 hypoxic and sub-oxic waters.

522 ii. a synthesis of these regional model analyses with those from global
523 biogeochemical models and Earth System Models. This will enable evaluation
524 of the relative contribution of the Arabian Sea and Bay of Bengal to global
525 oceanic N₂O emissions, and also provide mechanistic process knowledge to
526 inform the development of new biogeochemical parameterizations in the
527 global models towards improved predictive capability of N₂O-climate
528 feedbacks.

529

530 National and international collaboration will be an integral aspect of the envisioned
531 multidisciplinary studies. An improved understanding of the Indian Ocean nitrogen
532 cycle will contribute to our understanding of the crucial role of the nitrogen cycle in
533 societal-relevant issues such as climate change, eutrophication, air quality (pollution)
534 and the overall health of the ocean. To this end, we propose that nitrogen research
535 should be a continuing long-term focus of international research initiatives such as
536 the 2nd International Indian Ocean Expedition (IIOE-2: www.iioe-2.incois.gov.in),
537 SOLAS (Surface Ocean Lower Atmosphere Study: www.solas-int.org) and Future
538 Earth (www.futureearth.org).

539

540

541

542 Appendix A : Derivation of flux estimates for section 2

543 For the flux estimates calculated here, the Arabian Sea area is defined as the oceanic
544 region within the polygonal area bounded by (0°N, 42°E), (0°N, 76°E), (26.5°N, 76°E)
545 and (26.5°N, 59°E), and the Bay of Bengal as the region with bounds 5°-24°N and
546 76°-97.5°E.

547

548 Model derived atmospheric N-deposition and riverine N-fluxes : Atmospheric
549 inorganic nitrogen inputs are estimated from CAM version 3.5 model [Lamarque et
550 al., 2011]. Water soluble organic nitrogen (WSON) atmospheric deposition was
551 obtained from the Kanakidou et al. [2012] model. All global models have difficulties
552 in reproducing the spatial distribution of reduced and oxidized inorganic reactive
553 nitrogen deposition fluxes. In particular, in the northern Indian Ocean, global models
554 overestimated nitrate dry deposition fluxes while underestimating ammonium dry
555 deposition fluxes [Baker et al., 2017]. These discrepancies that can be partially
556 explained by seasonal biases in the sampling or by the pH dependence of the nitrate
557 and ammonium partitioning to the aerosol phase [Weber et al., 2016; Kanakidou et
558 al., 2018]. Riverine dissolved inorganic and organic nitrogen inputs were obtained
559 from the NEWS model [Seitzinger et al., 2010; Pedde et al. 2017] and other sources
560 listed in Table 1.

561

562 Flux estimates from aerosol data:

563 Data for nitrate (NO_3^-) and ammonium (NH_4^+) aerosol concentrations were obtained
564 from the Surface Ocean Lower Atmosphere Study (SOLAS) Project Integration
565 website

566 (http://www.bodc.ac.uk/solas_integration/implementation_products/group1/aerosol_rain/), and from sources cited in Table 1. The dry deposition fluxes of aerosol
567 WSON from the Arabian Sea were adopted from the mean value of the two cruises
568 sampled in Srinivas and Sarin [2013]. Given the aerosol concentration (C), the dry
569 deposition flux (F) was estimated using the following equation: $F = C \cdot V_d$, and by
570 assuming deposition velocities (V_d) of 1 cm s^{-1} for NO_3^- [Duce et al., 1991] and 0.6 cm
571 s^{-1} for NH_4^+ [Spokes et al., 2000]. The V_d is difficult to quantify and is affected by
572 several factors such as wind speed, surface roughness and, particle size etc. Due to
573 the inherent uncertainties associated with the assumed dry deposition velocities, the
574 estimates of atmospheric dry deposition of nitrogen carry additional uncertainty by
575 up to a factor of three.

577 Wet deposition is only collected at a few long-term coastal monitoring sites, and
578 hardly ever over the open ocean. Therefore, following Singh et al. [2012], wet
579 deposition fluxes (F_w) were estimated from the following formula:

580 $F_w = P \cdot S \cdot C_d \cdot \rho_a^{-1} \cdot \rho_w$, where P is the precipitation rate from the 1981-2010 Global
581 Precipitation Climatology Project long term mean [Adler et al., 2003], S is the
582 assumed scavenging ratio (330 and 200 for nitrate and ammonium, respectively
583 [Singh et al., 2012]), and 131 for WSON (the mean from Zamora et al. [2013]), C_d is
584 the aerosol concentration, and ρ_a and ρ_w are the densities of air and water,
585 respectively.

586 Interpolated values for each basin (the Arabian Sea and the Bay of Bengal) were
587 obtained at $1^\circ \times 1^\circ$ resolution), and then averaged to estimate wet and dry
588 deposition to the northern Indian Ocean.

589

590 **Appendix B : Global biogeochemistry models used in analysis of 3.1**

591 The investigations of Suntharalingam et al. [2012] and Jickells et al. [2017] both
 592 employed the PlankTOM ocean biogeochemistry model (PlankTOM5 and
 593 PlankTOM10 respectively) embedded in the NEMO ocean general circulation model,
 594 v 3.1 [Madec, 2008], and the diagnostic N₂O model of Suntharalingam et al. [2012].
 595 The model analysis of Landolfi et al. [2017] employed the UVic2.9 Earth System
 596 Model, and the N₂O parameterization of Zamora and Oschlies [2014]. The model
 597 analyses all evaluated the impact of changes in external nutrient input from the pre-
 598 industrial to the present, but have differences in their representation of the specific
 599 nutrient inputs considered (deposition, riverine and N₂ fixation), and in their
 600 parameterization of the nitrogen cycle. Further details of model specifications and
 601 assumptions are given in the individual publications.

602

603 **Appendix C: Estimation of N₂O Production and Impact of Nitrogen Deposition in
604 section 3.2**

605 For the regional model calculations of section 3.2, we derive a diagnostic estimate of
 606 the net N₂O source from the parameterizations of Suntharalingam et al. [2012, 2000]
 607 which estimate N₂O production as a function of organic matter remineralization via
 608 the local oxygen consumption rate. The N₂O production parameterizations are
 609 applied to the gridded biogeochemical model fields (specifically oxygen and oxygen
 610 utilization rates) of the high-resolution model simulations (1/12 degree) of
 611 Resplandy et al. [2012]. N₂O production is estimated from two separate pathways:
 612 (i) nitrification in the oxygenated open ocean, and (ii) higher N₂O yield processes
 613 (denitrification, enhanced nitrification) in low-oxygen zones. In addition, N₂O loss by
 614 denitrification is represented below a specified oxygen threshold ($[O_2] < [O_2]_{denit}$).
 615 Overall, the net N₂O production is estimated as:

$$616 \quad \text{Net N}_2\text{O production} = \alpha \cdot [\text{O}_2 \text{ consumption}] + \beta \cdot f(\text{O}_2) \cdot [\text{O}_2 \text{ consumption}] - [\text{Anoxic N}_2\text{O loss}]$$

617

618 Here, the scalar parameter α (mol [N₂O]/mol [O₂]) represents the N₂O yield from
 619 nitrification and is quantified from observed correlations between excess N₂O
 620 ($\Delta\text{N}_2\text{O}$) and Apparent Oxygen Utilization (AOU). The parameter β represents the
 621 higher yield of N₂O in sub-oxic zones, and $f(\text{O}_2)$ represents the non-linear functional
 622 dependence of N₂O yield on oxygen level. N₂O loss in anoxic conditions is
 623 represented as (-1) x the value of total N₂O production below oxygen threshold
 624 levels of $[O_2]_{denit}$; i.e., all N₂O produced in these zones is assumed to be consumed by
 625 denitrification processes, and this represents an upper bound on N₂O loss in these
 626 zones. For the analyses of this section we take the threshold level of $[O_2]_{denit}$ as 5
 627 $\mu\text{mol L}^{-1}$. Refer to Suntharalingam et al. [2012, 2000] and Buithenhuis et al. [2018]
 628 for additional details on the N₂O parameterization.

629 Table C1 presents the regionally aggregated results from the set of scenarios
 630 constructed for this analysis. These scenarios evaluate the sensitivity of estimated
 631 regional N₂O production to variation in the N₂O yield parameters α and β . The
 632 'Standard' model takes α and β values from Suntharalingam et al. [2012]. In addition
 633 we evaluate scenarios based on N₂O measurement analyses from the Arabian Sea
 634 (Law and Owens [1990], Naqvi and Noronha [1991], and Patra et al. [1999]). For
 635 these scenarios, the N₂O yield parameters were derived from the $\Delta\text{N}_2\text{O}/\text{AOU}$

636 correlations reported in the individual studies. Figure 1 presents the column
637 integrated distribution of N₂O production from the Standard scenario for the Arabian
638 Sea region.

639 We derive an empirical estimate of the impact of changes in nitrogen deposition in in
640 the Arabian Sea on regional N₂O production by applying the regionally averaged
641 fractional change in N₂O yield for the Arabian Sea region ($\gamma_{N_2O_{dep}}=0.125$) from the
642 nitrogen deposition of Suntharalingam et al. [2012] to the N₂O production estimates
643 derived above for the regional model:

644 i.e.,

$$\text{Change in N}_2\text{O} = (\gamma_{N_2O_{dep}}) \times [\text{N}_2\text{O production}]$$

647 **Table C1 : Regional model analysis of N₂O production scenarios and estimates of**
648 **the impact of nitrogen deposition**

649

N₂O Production Scenarios	N₂O Production (Tg N yr⁻¹) Nitrification Pathway	N₂O Production (Tg N yr⁻¹) Low-Oxygen Pathway	N₂O loss (Tg N yr⁻¹)	Net N₂O production (Tg N yr⁻¹)	Impact of Nitrogen Deposition on N₂O production* (Tg N yr⁻¹)
Standard $\alpha=0.75 \times 10^{-4}$; $\beta=0.01$	0.055	0.27	0.096	0.23	0.029
LOW $\alpha \beta$ scenario $\alpha=0.5 \times 10^{-4}$; $\beta=0.005$	0.037	0.135	0.048	0.124	0.015
HIGH $\alpha \beta$ scenario $\alpha=2.0 \times 10^{-4}$; $\beta=0.02$	0.147	0.54	0.124	0.564	0.070
Law and Owens 1990 LOW scenario $\alpha=0.33 \times 10^{-4}$; $\beta=0.01$	0.024	0.27	0.097	0.197	0.025
Law and Owens 1990 HIGH scenario $\alpha=3.1 \times 10^{-4}$; $\beta=0.01$	0.228	0.27	0.098	0.40	0.05
Naqvi and Noronha 1991 scenario $\alpha=1.7 \times 10^{-4}$; $\beta=0.01$	0.125	0.27	0.097	0.298	0.037
Patra 1999 scenario $\alpha=1.5 \times 10^{-4}$; $\beta=0.01$	0.110	0.27	0.097	0.283	0.036

650

651 *Impact of nitrogen deposition estimated as Change = $\gamma_{N_2O_{dep}} \times N_2O$ production

652

653

654 **Appendix D : Acronyms**

655 NCAR-CAM : National Center for Atmospheric Community Atmosphere Model

656 TM4-ECPL : Transport Model version 4-Environmental Chemical Processes
657 Laboratory

658 NEMO : Nucleus for European Modelling of the Ocean

659 PlankTOM : Plankton Types Ocean Model

660

661 **Acknowledgements :**

662 This paper resulted from the deliberations of GESAMP Working Group 38, the
663 Atmospheric Input of Chemicals to the Ocean. We thank the ICSU Scientific
664 Committee on Oceanic Research (SCOR), the US National Science Foundation (NSF),
665 the Global Atmosphere Watch (GAW) and the World Weather Research Program
666 (WWRP) of the World Meteorological Organization (WMO), the International
667 Maritime Organization (IMO), and the University of East Anglia for support of this
668 work. We acknowledge the British Oceanographic Data Centre (BODC) for
669 maintaining the SOLAS data integration website from which we used aerosol data for
670 the northern Indian Ocean. N₂O measurements from the AS and BoB are available
671 from the 'MarinE MethanE and NiTrous Oxide database' (MEMENTO:
672 <https://memento.geomar.de/de>). GPCP Precipitation data provided by the
673 NOAA/OAR/ESRL PSD, Boulder, Colorado, USA, from their Web site at
674 <https://www.esrl.noaa.gov/psd/>. E.B. and P.S acknowledge funding from the
675 European Union's Horizon 2020 research and innovation programme under grant
676 agreement No 641816 Coordinated Research in Earth Systems and Climate:
677 Experiments, kNowledge, Dissemination and Outreach (CRESCENDO).

678

679

680 **References**

681

682 Adler, R. F., Susskind, J., Huffman, G. J., Bolvin, D., Nelkin, E., Chang, A., Ferraro, R., Gruber,
683 A., Xie, P.-P., Janowiak, J., Rudolf, B., Schneider, U., Curtis, S. and Arkin, P., The version-2
684 global precipitation climatology project (GPCP) monthly precipitation analysis (1979-
685 present), *J. Hydrometeorol.*, 4(6), 1147–1167, 2003.

686 Attri, S. D. and Tyagi, A., *Climate Profile of India*, Met Monograph No. Environment
687 Meteorology-01/2010, New Delhi., 2010.

688 Babbin, A. R., Bianchi, D., Jayakumar, A., and Ward, B. B., Rapid nitrous oxide cycling in the
689 suboxic ocean, *Science*, 348(6239), 1127-1129, <https://doi.org/10.1126/science.aaa8380>,
690 2015.

691

692 Baker, A. R., Kanakidou, M., Altieri, K. E., Daskalakis, N., Okin, G. S., Myriokefalitakis, S.,
693 Dentener, F., Uematsu, M., Sarin, M. M., Duce, R. A., Galloway, J. N., Keene, W. C., Singh, A.,
694 Zamora, L., Lamarque, J.-F., Hsu, S.-C., Rohekar, S. S. and Prospero, J. M.: Observation- and
695 model-based estimates of particulate dry nitrogen deposition to the oceans, *Atmos Chem*
696 *Phys*, 17(13), 8189–8210, doi:10.5194/acp-17-8189-2017, 2017.

697 Bange, H. W., Andreae, M. O., Lal, S., Law, C. S., Naqvi, S. W. A., Patra, P. K., Rixen, T., and
698 Upstill-Goddard, R. C.: Nitrous oxide emissions from the Arabian Sea: A synthesis, *Atmos.*
699 *Chem. Phys.*, 1, 61-71, <https://doi.org/10.5194/acp-1-61-2001>, 2001.

700

701 Bange, H., Freing, A., Kock, A., and Loscher, C., *Marine pathways to Nitrous Oxide* 36-62,
702 *Nitrous Oxide and Climate Change*, Smith, K. (Ed.). London:
703 Routledge10.4324/9781849775113, 2010.

704

705 Bange, H., Naqvi, S. and Codispoti, L., The nitrogen cycle in the Arabian Sea. *Prog Oceanogr*
706 65: 145–158, 2005.

707

708 Banse, K., et al., Oxygen minimum zone of the open Arabian Sea: variability of oxygen and
709 nitrite from daily to decadal timescales, *Biogeosciences*, 11, 2237-2261,
710 <https://doi.org/10.5194/bg-11-2237-2014>, 2014.

711 Battaglia, G. and F. Joos, Marine N₂O Emissions From Nitrification and Denitrification
712 Constrained by Modern Observations and Projected in Multimillennial Global Warming
713 Simulations, *Glob. Biogeochem. Cycles*, 32 (1) , <https://doi.org/10.1002/2017GB005671>,
714 2018.

715

716 Bianchi, D., Dunne, J. P., Sarmiento, J. L. and Galbraith, E. D., Data-based estimates of
717 suboxia, denitrification, and N₂O production in the ocean and their sensitivities to dissolved
718 O₂, *Glob. Biogeochem. Cycles*, 26, 13 PP., doi:201210.1029/2011GB004209, 2012.

719 Bopp, L. et al., Multiple stressors of ocean ecosystems in the 21st century: projections with
720 CMIP5 models, *Biogeosciences* 10, 6225-6245, doi:10.5195/bg-10-6225-2013, 2013.

721

722 Bradley, E. S., Leifer, I., Roberts, D. A., Dennison, P. E. and Washburn, L.: Detection of marine
723 methane emissions with AVIRIS band ratios, *Geophys. Res. Lett.*, 38(10),
724 doi:10.1029/2011GL046729, 2011.

- 725 Bristow, L. A., et al. , N₂ production rates limited by nitrite availability in the Bay of Bengal
726 oxygen minimum zone, *Nature Geosci* 10(1): 24-29, 2017.
- 727 Buitenhuis, E., P. Suntharalingam and C. Le Quere, Constraints on global oceanic emissions
728 of N₂O from observations and models, *Biogeosciences*, 15, 2161-2175,
729 <https://doi.org/10.5194/bg-15-2161-2018>, 2018.
- 730 Capone, D. G., and Hutchins, D. A. ,Microbial biogeochemistry of coastal upwelling regimes
731 in a changing ocean. *Nat. Geosci.* 6, 711–717. doi: 10.1038/ngeo1916, 2013.
- 732 Ciais, P., et al., Carbon and Other Biogeochemical Cycles. In: *Climate Change 2013: The*
733 *Physical Science Basis. Contribution of Working Group I to the Fifth Assessment Report of*
734 *the Intergovernmental Panel on Climate Change [Stocker, T.F., D. Qin, G.-K. Plattner, M.*
735 *Tignor, S.K. Allen, J. Boschung, A. Nauels, Y. Xia, V. Bex and P.M. Midgley (eds.)]. Cambridge*
736 *University Press, Cambridge, United Kingdom and New York, NY, USA, 2013.*
737
- 738 Cocco, V. et al., Oxygen and indicators of stress for marine life in multi-model global
739 warming projections, *Biogeosciences* 10, 1849-1868, doi:10.5194/bg-10-1849-2013, 2013.
740
- 741 Codispoti, L., Brandes, J. A., Christensen, J. P., Devol, A., Naqvi, S. W. A., Paerl, H. W. and
742 Yoshinari, T., The oceanic fixed nitrogen and nitrous oxide budgets: Moving targets as we
743 enter the anthropocene?, *Scientia Marina*(65 (Suppl. 2)), 85–105, 2001.
- 744 Codispoti, L. A., Interesting times for marine N₂O, *Science*, 327, 1339–1340,
745 doi:10.1126/science.1184945, 2010.
746
- 747 Cohen, Y., and Gordon, L.I., Nitrous oxide production in the ocean, *J. Geophys. Res.*, 84,
748 347–353, doi:10.1029/JC084iC01p00347, 1979.
749
- 750 deCastro, M., M. C. Sousa, F. Santos, J. M. Dias and M. Gómez-Gesteira, How will Somali
751 coastal upwelling evolve under future warming scenarios? , *Nature Scientific Reports* 6,
752 Article number: 30137, 2016.
753
- 754 De Wilde, H.P.J., and Helder, W., Nitrous oxide in the Somali Basin: The role of upwelling.
755 *Deep Sea Research Part II: Topical Studies in Oceanography.* 44. 1319-1340. 10.1016/S0967-
756 0645(97)00011-8, 1997.
757
- 758 Dentener, F., et al., Nitrogen and sulfur deposition on regional and global scales: A
759 multimodel evaluation, *Glob. Biogeochem. Cycles*, 20(4),
760 <https://doi.org/10.1029/2005GB002672>, 2006.
- 761 Doney, S., et al., Impact of anthropogenic atmospheric nitrogen and sulfur deposition on
762 ocean acidification and the inorganic carbon system, *Proc .Natl. Acad. Sci., USA*, 104(37):
763 14580–14585, <https://doi.org/10.1073/pnas.0702218104> 2007.
764
- 765 Duce, R.A., et al., Impacts of atmospheric anthropogenic nitrogen on the open ocean,
766 *Science*, 320, Issue 5878, pp. 893-897 doi: 10.1126/science.1150369, 2008.
767
- 768 Frame, C. H., and K. L. Casciotti, Biogeochemical controls and isotopic signatures
769 of nitrous oxide production by a marine ammonia-oxidizing bacterium, *Biogeosciences*,
770 7(9), 2695–2709, doi:10.5194/bg-7-2695-2010, 2010.
771

- 772 Fowler, D., et al., The global nitrogen cycle in the twenty-first century. Philosophical
773 Transactions of the Royal Society B: Biological Sciences. 368(1621):20130164.
774 doi:10.1098/rstb.2013.0164, 2013.
775
- 776 Galloway, J. N., J. D. Aber, J.W. Erisman, S. P. Seitzinger, R.W. Howarth, E. B. Cowling, and B.
777 J. Cosby, The nitrogen cascade, *BioScience*, 53(4), 341–356, 2003.
778
- 779 Gandhi, N., Singh, A., Prakash, S., Ramesh, R., Raman, M., Sheshshayee, M., & Shetye, S.,
780 First direct measurements of N₂ fixation during a *Trichodesmium* bloom in the eastern
781 Arabian Sea. *Global Biogeochemical Cycles*, 25(4), 2011.
782
- 783 Garg, A., Shukla, P. R. and Kapshe, M., The sectoral trends of multigas emissions inventory of
784 India, *Atmos. Environ.*, 40(24), 4608–4620, doi:10.1016/j.atmosenv.2006.03.045, 2006.
785
- 786 Gnanadesikan, A., Dunne, J. P., and John, J.: Understanding why the volume of suboxic
787 waters does not increase over centuries of global warming in an Earth System Model,
788 *Biogeosciences*, 9, 1159–1172, doi:10.5194/bg-9-1159-2012, 2012.
789
- 790 Goes, J., P.G. Thoppil, H. do R Gomes, and J.T. Fasullo, Warming of the Eurasian Landmass Is
791 Making the Arabian Sea More Productive, *Science*, Vol. 308, Issue 5721, pp. 545-547
792 doi: 10.1126/science.1106610, 2005.
793
- 794 Gower, J., S. King and E. Young, Global remote sensing of *Trichodesmium*, *International*
795 *Journal of Remote Sensing*, Vol. 35, No. 14, 5459–5466,
796 <http://dx.doi.org/10.1080/01431161.2014.926422>, 2014.
797
- 798 Goreau, T. J., W. A. Kaplan, and S. C. Wofsy, Production of NO₂ and N₂O by nitrifying bacteria
799 at reduced concentrations of oxygen, *Applied and Environmental Microbiology*, 40(3), 526–
800 532, 1980.
801
- 802 Gruber, N., and Galloway, J.N., An Earth-system perspective of the global nitrogen cycle,
803 *Nature*, 451(7176), 293–296, doi:10.1038/nature06592, 2008.
804
- 805 Hood, R. R., Urban, E. R., McPhaden, M. J., Su, D., & Raes, E., The 2nd International Indian
806 Ocean Expedition (IIOE - 2): Motivating New Exploration in a Poorly Understood Basin.
807 *Limnology and Oceanography Bulletin*, 25(4), 117-124, 2016.
808
- 809 Ji, Q., Babbin, A. R., Jayakumar, A., Oleynik, S., and Ward, B. B. , Nitrous oxide production by
810 nitrification and denitrification in the eastern tropical south pacific oxygen minimum zone,
811 *Geophysical Research Letters*, 42(24), 10,755-710,764.
812 <https://doi.org/10.1002/2015GL066853>, 2015.
813
- 814 Jickells, T., et al., A re-evaluation of the magnitude and impacts of anthropogenic
815 atmospheric nitrogen inputs on the ocean, *Global Biogeochem. Cy.*, 31, 289–305,
816 <https://doi.org/10.1002/2016GB005586>, 2017.
- 817 Jyothibabu, R., Karnan, C., Jagadeesan, L., Arunpandi, N., Pandiarajan, R. S., Muraleedharan,
818 K. R. and Balachandran, K. K.: *Trichodesmium* blooms and warm-core ocean surface features
819 in the Arabian Sea and the Bay of Bengal, *Mar. Pollut. Bull.*, 121(1), 201–215,
820 doi:10.1016/j.marpolbul.2017.06.002, 2017.

- 821 Kanakidou, M., et al., Atmospheric fluxes of organic N and P to the global ocean, *Glob.*
822 *Biogeochem. Cycles*, 26(3), n/a–n/a, doi:10.1029/2011GB004277, 2012.
- 823 Kanakidou, M., Duce, R. A., Prospero, J. M., Baker, A. R., Benitez-Nelson, C., Dentener, F. J.,
824 Hunter, K. A., Liss, P. S., Mahowald, N., Okin, G. S., Sarin, M., Tsigaridis, K., Uematsu, M.,
825 Zamora, L. M. and Zhu, T.: Atmospheric fluxes of organic N and P to the global ocean, *Glob.*
826 *Biogeochem. Cycles*, 26(3), GB3026, doi:10.1029/2011GB004277, 2012.
- 827 Kanakidou, M., et al., Past, Present, and Future Atmospheric Nitrogen Deposition, *J.*
828 *Atmospheric Sci.*, 73(5), 2039–2047, doi:10.1175/JAS-D-15-0278.1, 2016.
- 829 Kanakidou, M., Myriokefalitakis, S., Tsigaridis, K., Aerosols in atmospheric chemistry and
830 biogeochemical cycles of Nutrients, *Environ. Res. Lett.* 13 063004, 2018.
- 831
832 Kock, A., et al., Extreme N₂O accumulation in the coastal oxygen minimum zone off Peru,
833 *Biogeosci.* 13(3): 827-840, 2016.
- 834 Krishna, M. S., et al., Export of dissolved inorganic nutrients to the northern Indian Ocean
835 from the Indian monsoonal rivers during discharge period, *Geochimica et Cosmochimica*
836 *Acta* 172: 430-443, 2016.
- 837 Krishnamurthy, A., J.K. Moore, C. Luo, C.S. Zender, The effects of atmospheric inorganic
838 nitrogen deposition on ocean biogeochemistry, *JGR-Biogeosciences*, 112, G02019,
839 <https://doi.org/10.1029/2006JG000334>, 2007.
- 840
841 Krishnamurthy, J.K. Moore, N. Mahowald, C. Luo, S.C. Doney, K. Lindsay C.S. Zender,
842 Impacts of increasing anthropogenic soluble iron and nitrogen deposition on ocean
843 biogeochemistry, *Glob. Biogeochem. Cycles*, 23(3), doi.org/10.1029/2008GB003440, 2009.
- 844 Lachkar, Z., Lévy, M., and Smith, S.: Intensification and deepening of the Arabian Sea oxygen
845 minimum zone in response to increase in Indian monsoon wind intensity, *Biogeosciences*,
846 15, 159-186, <https://doi.org/10.5194/bg-15-159-2018>, 2018.
- 847 Lamarque, J.-F., Kyle, G. P., Meinshausen, M., Riahi, K., Smith, S. J., Vuuren, D. P. van, Conley,
848 A. J. and Vitt, F., Global and regional evolution of short-lived radiatively-active gases and
849 aerosols in the Representative Concentration Pathways, *Clim. Change*, 109(1–2), 191–212,
850 doi:10.1007/s10584-011-0155-0, 2011.
- 851 Lal, S., and P. Patra, Variabilities in the fluxes and annual emissions of nitrous oxide from the
852 Arabian Sea, *Glob. Biogeochem. Cycles*, Vol. 12, 2, pp. 321-327, 1998.
- 853
854 Lamarque, J.-F., et al., Multi-model mean nitrogen and sulfur deposition from the
855 Atmospheric Chemistry and Climate Model Intercomparison Project (ACCMIP): evaluation
856 historical and projected changes, *Atmospheric Chem. Phys. Discuss.*, 13(3), 6247–6294,
857 doi:10.5194/acpd-13-6247-2013, 2013.
- 858
859 Landolfi, A., Dietze, H., Koeve, W. and Oschlies, A., Overlooked runaway feedback in the
860 marine nitrogen cycle: the vicious cycle, *Biogeosciences*, 10(3), 1351–1363, doi:10.5194/bg-
861 10-1351-2013, 2013.
- 862
863 Landolfi, A., Somes, C., Koeve, W., Zamora, L. M., Oschlies, A., Oceanic nitrogen cycling and
864 N₂O flux perturbations in the Anthropocene, *Glob. Biogeochem. Cycles*, 2017.

- 865
866 Law, C. S. and Owens, N. J. P., Significant flux of atmospheric nitrous oxide from the
867 northwest Indian Ocean, 346(6287), 826–828, 1990.
- 868 Liu, K. K., Seitzinger, S. P. and Mayorga, E.: Fluxes of Nutrients and Selected Organic
869 Pollutants Carried by Rivers, in In: Urban ER, Sundby B., Rizzoli P. et al. (ed) Watersheds,
870 bays, and bounded seas: The science and management of semi-enclosed marine systems,
871 pp. 141–167, Island Press, Washington, D. C., 2008.
- 872 Löscher, C. R., et al., Production of oceanic nitrous oxide by ammonia-oxidizing archaea,
873 *Biogeosci.* 9: 2419-2429, 2012.
- 874 Madec, G., NEMO ocean engine, Note du Pôle de modélisation, Institut Pierre-Simon Laplace
875 (IPSL), France, No 27, ISSN No 1288-1619, 2008.
- 876 Madhupratap, M., S. Prasanna Kumar, P. M. A. Bhattathiri, M. Dileep Kumar, S. Raghukumar,
877 K. K. C. Nair, and N. Ramaiah,, Mechanism of the biological response to winter cooling in the
878 northeastern Arabian Sea, *Nature*, 384, 549–552, doi:10.1038/384549a0, 1996.
- 879 Martin, J. H., Knauer, G. A., Karl, D. M. and Broenkow, W. W., VERTEX: carbon cycling in the
880 northeast Pacific, *Deep Sea Res. Part Oceanogr. Res. Pap.*, 34(2), 267–285,
881 doi:10.1016/0198-0149(87)90086-0, 1987.
- 882 Martin, G. D., Nisha, P. A., Balachandran, K. K., Madhu, N. V., Nair, M., Shaiju, P., Joseph, T.,
883 Srinivas, K. and Gupta, G. V. M.: Eutrophication induced changes in benthic community
884 structure of a flow-restricted tropical estuary (Cochin backwaters), India, *Environ. Monit.*
885 *Assess.*, 176(1–4), 427–438, doi:10.1007/s10661-010-1594-1, 2011.
- 886 Martino, M., D. Hamilton A. R. Baker T. D. Jickells T. Bromley Y. Nojiri B. Quack P. W.
887 Boyd, Western Pacific atmospheric nutrient deposition fluxes, their impact on surface ocean
888 productivity, *Glob. Biogeochem. Cycles*, 28(7), doi.org/10.1002/2013GB004794, 2014.
889
- 890 McCreary, J.P., Z. Yu, R.R. Hood, P.N. Vinayachandran, R. Furue, A. Ishida, and K.J. Richards.
891 2013. Dynamics of the Indian-Ocean oxygen minimum zones. *Progress in Oceanography* 112-
892 113:15-37. Naqvi, S. W. A., Jayakumar, D. A., Narvekar, P. V., Naik, H., Sarma, V. V. S. S.,
893 D'Souza, W., Joseph, S. and George, M. D., Increased marine production of N₂O due to
894 intensifying anoxia on the Indian continental shelf, *Nature*, 408(6810), 346–349, 2000.
- 895 Montoya, J. P., Voss, M., Kahler, P. and Capone, D. G.: A Simple, High-Precision, High-
896 Sensitivity Tracer Assay for N₂ Fixation, *Appl. Environ. Microbiol.*, 62(3), 986–993, 1996.
897
- 898 Moore, J.K., and S.C. Doney, Iron availability limits the ocean nitrogen inventory stabilizing
899 feedbacks between marine denitrification and nitrogen fixation, *Glob. Biogeochem. Cycles*,
900 21(2), doi.org/10.1029/2006GB002762, 2007.
901
- 902 Morrison, J.M., L.A. Codispoti, S.L. Smith, K. Wishner, C. Flagg, W.D. Gardner, S. Gaurin,
903 S.W.A. Naqvi, V. Manghnani, L. Prosperie, and J.S. Gundersen, The oxygen minimum zone in
904 the Arabian Sea during 1995. *Deep-Sea Research, Part II* 46(8-9):1903-1931,1999.
905
- 906 Naqvi, S. W. A. and Noronha, R. J., Nitrous oxide in the Arabian Sea, *Deep-Sea Res.*, 38, 871–
907 890, 1991.
908

- 909 Naqvi, S. W. A., et al., Nitrous oxide in the western Bay of Bengal, *Mar. Chem.* **47**: 269-278,
910 1994.
- 911
- 912 Naqvi, S. W. A., Yoshinari, T., Jayakumar, D. A., Altabet, M. A., Narvekar, P. V., Devol, A. H.,
913 Brandes, J. A., and Codispoti, L. A.: Budgetary and biogeochemical implications of N₂O
914 isotope signatures in the Arabian Sea, *Nature*, 394, 462–464, 1998.
- 915
- 916 Naqvi, S. W. A., Jayakumar, D. A., Narveka, P. V., Naik, H., Sarma, V. V. S. S., D'Souza, W.,
917 Joseph, S., and George, M. D.: Increased marine production of N₂O due to intensifying anoxia
918 on the Indian continental shelf, *Nature*, 408, 346–349, 2000.
- 919
- 920 Naqvi, S.W.A., Jayakumar D.A. , P.V. Narvekar, H. Naik, Sarma, V.V.S.S., D'Souza, W.,
921 Joseph, S., and George, M.D., Marine hypoxia/anoxia as a source of CH₄ and N₂O.
922 *Biogeosciences* 7:2159-2190, 2010a.
- 923
- 924 Naqvi, S. W. A., et al. , Carbon and nitrogen fluxes in the northern Indian Ocean. In: Carbon
925 and nutrient fluxes in continental margins: A global synthesis. K.-K. Liu, L. Atkinson, R.
926 Quiñones and L. Talaue-McManus. New York, Springer-Verlag: 180-191, 2010b.
- 927
- 928 Patra, P., S. Lal, S. Venkataramani, S.N. de Sousa, V.V.S.S. Sarma, and S. Sardesai, Seasonal
929 and spatial variability in N₂O distribution in the Arabian Sea, *Deep-Sea Research I* 46, pp. 529-
930 543, 1999.
- 931
- 932 Paulmier, A. and Ruiz-Pino, D., Oxygen Minimum Zones (OMZs) in the modern ocean, *Prog.*
933 *Oceanogr.*, 80(3–4), 113–128, doi:10.1016/j.pocean.2008.05.001, 2008.
- 934
- 935 Paulmier, A., Kriest, I., and Oschlies, A., Stoichiometries of remineralisation and
936 denitrification in global biogeochemical ocean models, *Biogeosciences*, 6, 923–935,
937 doi:10.5194/bg-6-923-2009, 2009.
- 938
- 939 Pedde, A., Kroeze, C., Mayorga, E., Seitzinger, S.P., Modeling sources of nutrients in rivers
940 draining into the Bay of Bengal - a scenario analysis, *Reg. Environ. Change*, 17:2495-2506,
941 2017.
- 942
- 943 Ramanathan, V., C. Chung, D. Kim, T. Bettge, L. Buja, J. T. Kiehl, W. M. Washington, Q. Fu, D.
944 R. Sikka, M. Wild, Atmospheric brown clouds: Impacts on South Asian climate and
945 hydrological cycle, *Proceedings of the National Academy of Sciences*, 102 (15) 5326-5333;
946 doi: 10.1073/pnas.0500656102, 2005.
- 947
- 948 Ramesh, R., Paneer Selvam, A., Robin, R. S., Ganguly, D., Singh, G. and Purvaja, R.: 23 -
949 Nitrogen Assessment in Indian Coastal Systems, in *The Indian Nitrogen Assessment*, edited
950 by Y. P. Abrol, T. K. Adhya, V. P. Aneja, N. Raghuram, H. Pathak, U. Kulshrestha, C. Sharma,
and B. Singh, pp. 361–379, Elsevier, 2017.
- 951
- 952 Rao, G. D., et al., Distribution and air-sea exchange of nitrous oxide in the coastal Bay of
Bengal during peak discharge (southwest monsoon), *Mar. Chem.* 155: 1-9, 2013.
- 953
- 954 Resplandy, L., Lévy, M., Madec, G., Pous, S., Aumont, O. and Kumar, D., Contribution of
mesoscale processes to nutrient budgets in the Arabian Sea, *J. Geophys. Res. Oceans*,
955 116(C11), n/a–n/a, doi:10.1029/2011JC007006, 2011.

- 956 Resplandy, L., Lévy, M., Bopp, L., Echevin, V., Pous, S., Sarma, V. V. S. S. and Kumar, D.,
957 Controlling factors of the oxygen balance in the Arabian Sea's OMZ, *Biogeosciences*, 9(12),
958 5095–5109, doi:10.5194/bg-9-5095-2012, 2012.
- 959 Safai, P. D., Rao, P. S. P., Momin, G. A., Ali, K., Chate, D. M. and Praveen, P. S.: Chemical
960 composition of precipitation during 1984–2002 at Pune, India, *Atmos. Environ.*, 38(12),
961 1705–1714, doi:10.1016/j.atmosenv.2003.12.016, 2004.
- 962 Sattar, M. A., et al. , The increasing impact of food production on nutrient export by rivers
963 to the Bay of Bengal 1970-2050, *Mar. Poll. Bull.* 80(1-2): 168-178, 2014.
- 964 Schott, F. A. and McCreary, J. P. The monsoon circulation of the Indian Ocean, *Prog.*
965 *Oceanogr.* 51, 1–123, 2001.
- 966 Singh, A., and Ramesh, R., Contribution of riverine dissolved inorganic nitrogen flux to new
967 production in the coastal northern Indian Ocean: An assessment. *International Journal of*
968 *Oceanography*, 2011.
- 969
970 Singh, A., Gandhi, N. and Ramesh, R., Contribution of atmospheric nitrogen deposition to
971 new production in the nitrogen limited photic zone of the northern Indian Ocean, *J.*
972 *Geophys. Res.*, 117(C6), doi:10.1029/2011JC007737, 2012.
- 973
974 Singh, A., and Ramesh, R. Environmental Controls on New and Primary Production in the
975 Northern Indian Ocean. *Progress in Oceanography* 131: 138–145, 2015.
- 976
977 Seitzinger, S. P., Mayorga, E., Bouwman, A. F., Kroeze, C., Beusen, A. H. W., Billen, G., Van
978 Drecht, G., Dumont, E., Fekete, B. M., Garnier, J. and Harrison, J. A.: Global river nutrient
979 export: A scenario analysis of past and future trends, *Glob. Biogeochem. Cycles*, 24(4),
980 GB0A08, doi:10.1029/2009GB003587, 2010.
- 981
982 Somes, C. J., Landolfi, A., Koeve, W., and Oschlies, A., Limited impact of atmospheric
983 nitrogen deposition on marine productivity due to biogeochemical feedbacks in a global
984 ocean model, *Geophys. Res. Lett.*, 43, 4500, doi:10.1002/2016GL068335, 2016.
- 985
986 Spokes, L. J., Yeatman, S., Cornell, S. E., and Jickells, T. D., Nitrogen deposition to the
987 eastern Atlantic Ocean, The importance of south-easterly flow, *Tellus*, 52B, 37 – 49, 2000.
- 988 Srinivas, B. and Sarin, M. M., Atmospheric deposition of N, P and Fe to the Northern Indian
989 Ocean: Implications to C- and N-fixation, *Sci. Total Environ.*, 456–457, 104–114,
990 doi:10.1016/j.scitotenv.2013.03.068, 2013.
- 991 Srinivas, B., Sarin, M. M. and Sarma, V. V. S. S.: Atmospheric dry deposition of inorganic and
992 organic nitrogen to the Bay of Bengal: Impact of continental outflow, *Mar. Chem.*, 127(1–4),
993 170–179, doi:10.1016/j.marchem.2011.09.002, 2011.
- 994 Stramma, L., S. Schmidtko, L. A. Levin, G. C. Johnson, G. C., Ocean oxygen minima expansions
995 and their biological impacts. *Deep-Sea Res. Pt. I*, 57 (4), 587- 595, 2010.
- 996
997 Stramma, L., A. Oschlies, S. Schmidtko, Mismatch between observed and modeled
998 848 trends in dissolved upper-ocean oxygen over the last 50 yr, *Biogeosciences*, 9 (10),
999 doi:10.5194/bg-9-4045-2012, 2012.

- 1001 Suntharalingam, P., J. L. Sarmiento, and J. R. Toggweiler, Global significance of nitrous-oxide
1002 production and transport from oceanic low-oxygen zones: A modeling study, *Global*
1003 *Biogeochem. Cycles*, 14(4), 1353–1370, doi:10.1029/1999GB900100, 2000.
- 1004 Suntharalingam, P., Buitenhuis, E., Quéré, C. L., Dentener, F., Nevison, C., Butler, J. H., Bange,
1005 H. W. and Forster, G.: Quantifying the impact of anthropogenic nitrogen deposition on
1006 oceanic nitrous oxide, *Geophys. Res. Lett.*, 39, doi:201210.1029/2011GL050778, 2012.
- 1007 Thorpe, A. K., Roberts, D. A., Dennison, P. E., Bradley, E. S. and Funk, C. C.: Point source
1008 emissions mapping using the Airborne Visible/Infrared Imaging Spectrometer (AVIRIS),
1009 edited by S. S. Shen and P. E. Lewis, pp. 839013-839013–9., 2012.
- 1010 Van Mooy, B. A. S., Keil, R. G. and Devol, A. H., Impact of suboxia on sinking particulate
1011 organic carbon: Enhanced carbon flux and preferential degradation of amino acids via
1012 denitrification, *Geochim. Cosmochim. Acta*, 66(3), 457–465, doi:10.1016/S0016-
1013 7037(01)00787-6, 2002.
- 1014 Vet, R., et al., A global assessment of precipitation chemistry and deposition of sulfur,
1015 nitrogen, sea salt, base cations, organic acids, acidity and pH, and phosphorus, *Atmos.*
1016 *Environ.*, 93, 3–100, doi:10.1016/j.atmosenv.2013.10.060, 2014.
- 1017 von Glasow, R., T. D. Jickells, A. Baklanov, G. R. Carmichael, T. M. Church, L. Gallardo, C.
1018 Hughes, M. Kanakidou, P. S. Liss, L. Mee, R. Raine, P. Ramachandran, R. Ramesh, K.
1019 Sundseth, U. Tsunogai, M. Uematsu, T. Zhu, Megacities and Large Urban Agglomerations in
1020 the Coastal Zone: Interactions Between Atmosphere, Land, and Marine Ecosystems
1021 *Ambio*, 42, 13-28, 2013.
- 1022
1023 Ward, B. B. , A. H. Devol, J. J. Rich, B. X. Chang, S. E. Bulow, Hema Naik, Anil Pratihary & A.
1024 Jayakumar, Denitrification as the dominant nitrogen loss process in the Arabian Sea, *Nature*
1025 volume 461, pages 78–81, 2009.
- 1026
1027 Weber, T., and Deutsch, C., Local versus basin-scale of marine nitrogen fixation. *Proc. Natl*
1028 *Acad. Sci. USA* 111, 8741-8746, 2014.
- 1029
1030 Weber, R. J., Guo, H., Russel, I. A. G., Nenes, A., High aerosol acidity despite declining
1031 atmospheric sulfate concentrations over the past 15 years, *Nat. Geosci.* 9 282–5, 2016.
- 1032
1033 Wiggert, J. D., B.H. Jones, T.D. Dickey, K.H. Brink, R.A. Weller, J.Marra, L.A. Codispoti, The
1034 Northeast Monsoon's impact on mixing, phytoplankton biomass and nutrient cycling in the
1035 Arabian Sea, *Deep Sea Research Part II: Topical Studies in Oceanography*, vol. 47, issue 7-8,
1036 pp. 1353-1385, doi.org/10.1016/S0967-0645(99)00147-2, 2000.
- 1037
1038 Yang, S., and N. Gruber, The anthropogenic perturbation of the marine nitrogen cycle by
1039 atmospheric deposition: Nitrogen cycle feedbacks and the ¹⁵N Haber-Bosch effect, *Global*
1040 *Biogeochem. Cycles*, 30(10), 1418-1440, doi:10.1002/2016GB005421, 2016.
- 1041
1042 Zamora, L. M. and Oschlies, A., Surface nitrification: A major uncertainty in marine N₂O
1043 emissions, *Geophys. Res. Lett.*, 41(12), 2014GL060556, doi:10.1002/2014GL060556, 2014.
- 1044
1045 Zamora, L. M., J. Prospero, D. Hansell, and J. M. Trapp, Atmospheric P deposition to the
1046 subtropical North Atlantic: sources, properties, and relationship to N deposition. *Journal of*
Geophysical Research- Atmospheres, 1546-1562, doi:10.1002/jgrd.50187, 2013.

1047

1048 Zamora, L. M., Oschlies, A., Bange, H. W., Huebert, K. B., Craig, J. D., Kock, A. and Löscher, C.
1049 R., Nitrous oxide dynamics in low oxygen regions of the Pacific: insights from the MEMENTO
1050 database, *Biogeosciences*, 9(12), 5007–5022, doi:10.5194/bg-9-5007-2012, 2012.

ACCEPTED MANUSCRIPT

Table 1. Estimates of present-day external(non-recycled) dissolved nitrogen inputs (Tg N yr⁻¹) to the Arabian Sea and Bay of Bengal from riverine, atmospheric, and diazotrophic sources.

	Riverine	Atmospheric	N ₂ Fixation
Arabian Sea			
Model-derived	0.4 ^a	1.4 ^d	2.6 ^f -6.2 ^g
Obs-based	0.1-0.4 ^b	1.8 ^e	0.0-20.4 ^{h,i}
Bay of Bengal			
Model-derived	5 ^a	1.1 ^d	4.2 ^f -4.3 ^g
Obs-based	0.9-2.0 ^c	1.6 ^e	0.6-11.3 ⁱ

^aThis study, year 2000 model output includes dissolved organic and inorganic nitrogen [Seitzinger et al. 2010; Pedde et al. 2017]

^b[Singh and Ramesh, 2011]; [Singh et al., 2012]

^c[Srinivas and Sarin, 2013] and references therein.

^dThis study, year 2005 model output includes water soluble inorganic and organic nitrogen [Lamarque et al., 2011; Kanakidou et al., 2012]; See Appendix A for further details.

^eThis study, see Appendix A for further details.

^f[Jickells et al. 2017]

^g[Le Quéré et al 2016]

^h[Gandhi et al., 2011] estimated N₂ fixation rates using ¹⁵N₂ with less than 6% uncertainty.

ⁱ[Srinivas and Sarin, 2013] and references therein, converted to the larger open ocean regions used in this study (6.6x10⁶ km² for the Arabian Sea, and 3.0x10⁶ km² for the Bay of Bengal). Nitrogen fixation rates were estimated with respect to atmospheric inputs by assuming Fe and P limitation in the ocean.

Table 2 : Model-derived estimates of changes in global and northern Indian ocean N₂O production due to the impact of external nitrogen inputs from atmospheric deposition. Estimates shown summarize results from the model analyses of Suntharalingam et al. [2012], Jickells et al. [2017], and the NDEP simulation of Landolfi et al. [2017].

REGION	Present day oceanic N ₂ O source * (Tg N yr ⁻¹)	Change in N ₂ O source due to nitrogen inputs (pre-industrial to present day) (Tg N yr ⁻¹)
Northern Indian Ocean**	0.3 – 0.6	0.003 – 0.05
Global Ocean	2.5-4.5	0.04 – 0.15

* Present day values derived from model simulations for period 1995-2005.

** Defined here as the ocean region north of the Equator and within the longitudinal range 42°E-100°E.

Figure 1. Net column-integrated N₂O production (units : Mg N m⁻² yr⁻¹) in the Arabian Sea derived from the regional high-resolution model analysis reported in section 3.2. The net N₂O production is derived from the methodology outlined in Appendix C and is the sum of N₂O production from the nitrification and low-oxygen pathways, and N₂O loss below an oxygen threshold of 5 μmol L⁻¹.

Figure 2 : Illustration of the possible ratio of net nitrogen loss: net nitrogen gain (mol:mol) from atmospheric nitrogen deposition to OMZs in the northern Indian Ocean assuming either a) the Martin curve, or b) the Van Mooy curve. Calculations based on World Ocean Atlas O₂ data [Bianchi et al. 2012].

ACCEPTED MANUSCRIPT

Figure 1. Net column-integrated N_2O production (units : $\text{Mg N m}^{-2} \text{ yr}^{-1}$) in the Arabian Sea derived from the regional high-resolution model analysis reported in section 3.2. The net N_2O production is derived from the methodology outlined in Appendix C and is the sum of N_2O production from the nitrification and low-oxygen pathways, and N_2O loss below an oxygen threshold of $5 \mu\text{mol L}^{-1}$.

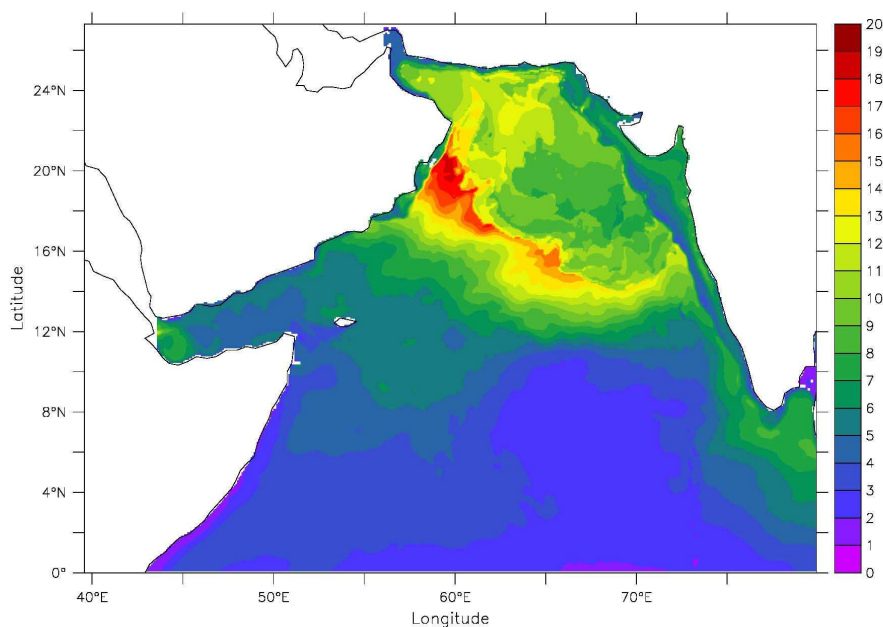


Figure 2 : Illustration of the possible ratio of net nitrogen loss: net nitrogen gain (mol:mol) from atmospheric nitrogen deposition to OMZs in the northern Indian Ocean assuming either a) the Martin curve, or b) the Van Mooy curve. Calculations based on World Ocean Atlas O₂ data [Bianchi et al. 2012].

